ResearchGate

See discussions, stats, and author profiles for this publication at: https://www.researchgate.net/publication/268983408

Combining Numerical Methods for Basin and Turbine Scales for Improved Modelling of in-situ Turbine Arrays

Conference Paper · September 2013

CITATIONS
8

READS
151

4 authors:

Michael Shives
University of Victoria
10 PUBLICATIONS **321** CITATIONS
SEE PROFILE

Curran Crawford
University of Victoria
173 PUBLICATIONS **2,980** CITATIONS
SEE PROFILE

Clayton E. Hiles
Kerr-Wood-Leidal Consulting Engineers
17 PUBLICATIONS **319** CITATIONS
SEE PROFILE

Roy A. Walters
no affiliation
101 PUBLICATIONS **4,844** CITATIONS
SEE PROFILE

Some of the authors of this publication are also working on these related projects:

Developing Yield Prediction Methods for Tidal Farms; Including Wake Interaction effects View project

AWESCO - Airborne Wind Energy System Modelling, Control and Optimisation View project

All content following this page was uploaded by Clayton E. Hiles on 18 August 2015.

The user has requested enhancement of the downloaded file.

Combining Numerical Methods for Basin and Turbine Scales for Improved Modelling of in-situ Turbine Arrays

Michael Shives*, Curran Crawford*, Clayton Hiles† and Roy Walters†
*Dept. of Mech. Eng., University of Victoria, BC. Canada
E-mail: mrshives@uvic.ca, curranc@uvic.ca
†Cascadia Coast Research , Victoria, BC. Canada
E-mail: clayton@cascadiacoast.com

***Abstract*—This paper proposes an approach for combining device-scale and basin-scale simulation methods to provide realistic in-situ performance analysis of turbine arrays and with the eventual goal of determining basin-scale effects from large turbine arrays. The present state-of-the-art basin-scale simulation methods represent turbines as sub-grid-scale objects, typically using semi-empirical/semi-analytical turbine models. Device-scale CFD simulation methods can resolve flows around turbines and can predict turbine performance outside the idealized assumptions of analytical methods. Thus, combining the capabilities of these two types of simulations is desirable for accurate in-situ performance analysis with the correct influence of turbines on the basin flow. The approach is to parameterize turbine thrust and power using a reference velocity available to both types of model. This is a volume average over a region in space that can be resolved by the basin-scale model. The approach is accurate provided both methods predict a consistent reference velocity. This paper presents preliminary studies testing such consistency for simplified channel scenarios, finding that as long as the averaging volume has length scales twice the turbine diameter, relative error in power is typically under ≈5%. When applied to a complex real-world flow, the relative error was larger. It is thought that at present, the method is suitable for approximate power prediction and further improvement is required for accurate turbine performance studies.**

***Index Terms*—Tidal Turbine, Array, CFD, RiCOM, basin-scale, Bay of Fundy, Minas Passage, Porous Disk, Actuator Disk**

I. Introduction

Tidal turbine technology is progressing from prototypes and demonstrators to commercial applications. Developers are transitioning from isolated turbines to small arrays of turbines (such as the proposed three-rotor design by Marine Current Turbines) and once the technology proves economically viable, to large arrays of many turbines. There is presently a requirement to develop methods to simulate arrays of turbines and to optimize the layout of turbines for a given site. For small arrays, a predictive capability for the mutual influence of turbines on each other will be required. Additionally, the influence of tidal flow boundaries (i.e. channel bottom, free surface, and lateral bounds) should be resolved. For larger arrays, it will also be necessary to predict the influence of the turbines on basin dynamics.

Presently, simulation methods for tide-driven basin-scale flows exist and have been validated with good agreement to measured data in the absence of turbines. These have been used to model the effect of large arrays of turbines on basin scale flows (e.g. [1]). Such methods have used semi-analytical/semi-empirical representations of turbines which typically limited to idealized flows (such as uniform inflow, 2D flow, empirical wake models, etc.), thus such methods can only provide rough estimates for power generation. Due to the maximum resolution (10s of meters) of basin-scale models, they cannot resolve the mutual influence of turbines on each other, and their predictive capability for the influence of the flow boundaries on turbine performance remains to be assessed.

At the device scale, CFD simulation can be used to model turbines for a wide range of inflow conditions and can resolve mutual influences between turbines and influences of local bathymetry. With such simulations, is it possible to accurately simulate a wide range of array configurations but the computational expense can become very large. While there have been some applications of CFD to entire basin-scale flows, such an approach may be too computationally expensive. It is likely that since dedicated basin scale models use a reduced set of equations compared to general-purpose CFD solvers, they should run faster. They should also be more accurate for basin-dynamics since they use turbulence parameterizations specific to basin-scale flows which are different from typical CFD codes.

This paper presents work done towards combining the capabilities of basin-scale simulation methods with device-scale methods to obtain an overall approach which allows accurate in-situ performance analysis for turbines. It is thought that such a methodology could evolve to a point where it becomes possible to simulate large arrays of turbines with accurate power predictions and an accurate prediction of the back-effects on the tidal flow regime.

II. Overall Approach

The proposed approach is depicted in figure 1 and consists of the following steps. First, the basin-scale simulation is

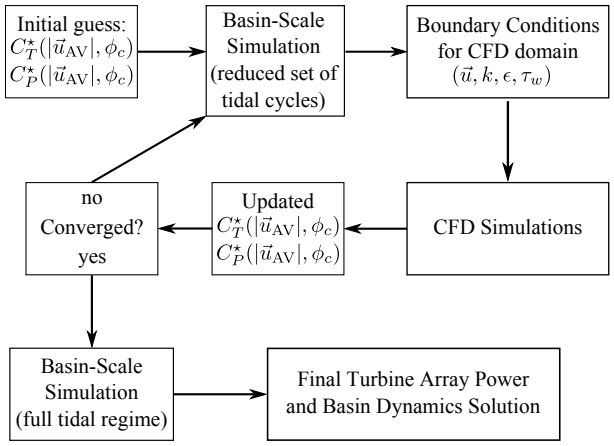

Fig. 1. Flow Chart of Proposed Methodology

used to predict the natural tidal flow throughout the channel. Then, potential turbine sites are chosen and CFD meshes are developed for sub-domains containing single turbines, or groups of turbines. Then an iterative process begins to develop a performance model for each turbine in the array. CFD simulations are run on the sub-domains to predict the mutual influence of the turbines on each other, as well as the influences of local bathymetry. It would be computationally expensive to run a transient CFD simulation of an entire tidal cycle. However, it is likely valid to make a quasi-steady assumption and to run several steady-state CFD simulations at different phases of the tidal cycle. The CFD simulations are used to determine non-dimensional turbine performance parameters $C_T^\star$ and $C_P^\star$. Note that $C_T^\star$ and $C_P^\star$ may vary throughout the tidal cycle due to changes in flow speed ($|\vec{u}_{\mathrm{AV}}|$) or direction (ϕ), or due to the turbine control strategy, so the performance model would involve curve-fitting. Next, a new basin-scale simulation is run with the turbine forces added. This generates new boundary conditions for the CFD simulations, and the entire process is iterated until convergence of $C_T^\star$ and $C_P^\star$, resulting in the final empirical turbine model. Then, the final parameterization can be used in the basin-scale simulation for more in depth studies of longer duration[1].

III. Analysis Codes

This section gives a brief overview of the analysis codes employed, for further detail please refer to the supplied references (for RiCOM) or product documentation (for CFX). In general, basin-scale methods typically solve the shallow water equations, while CFD solvers solve the full 3D RANS equations. Both classes of model employ turbulence closures (commonly k-ϵ) but with different coefficients which have been tuned for different classes of flows and differing typical grid resolution.

[1]A 'tighter' coupling between CFD and basin-scale methods is also possible, where the two models share boundaries and simulations run over entire tidal cycles, but presently this approach has not been attempted due to the programming complexity and computational cost.

A. Basin-Scale

For the basin-scale simulations, the River and Coastal Ocean Model (RiCOM) developed by Dr. Roy Walters was used. A brief general description of the model is provided here with greater detail in [2]–[5]. RiCOM is formulated in rotating frame of reference using the Reynolds-averaged Navier-Stokes equations and the Boussinesq approximation. The equations are also spatially averaged to derive double-averaged equations that allow sub-grid spatial effects (vegetation, bottom roughness, etc.) to be included in a rigorous manner [4]. This double averaging provides a means to couple the results of small-scale CFD models with the large-scale Ocean model.

RiCOM solves the primitive hydrodynamic equations with a semi-implicit time-stepping scheme that is unconditionally stable with respect to time-step size, which allows the time-step size to be chosen to adequately resolve the temporal variation of the flow without numerical stability constraints. The model uses a semi-Lagrangian approximation for advection that is accurate, stable, and robust which yields accurate results without oscillations for high speed flows such as occur over weirs, in flow constrictions, and tidal rapids. A finite element spatial approximation is used, giving considerable flexibility in designing the computational grid [5]. Wetting and drying capabilities are inherent to the finite volume continuity equation employed and the model conserves mass both locally and globally.

B. Device-Scale

The device-scale simulations used the commercially available ANSYS CFX software. CFX solves the Reynolds-averaged-Navier-Stokes equations using finite-volume discretization. The *high resolution* advection scheme was used, which blends 2nd order central differencing with 1st order upwind schemes, and favours central differencing unless upwinding is required for simulation stability. CFX uses a co-located grid and avoids even-odd decoupling with a modified Rhie/Chow interpolation. The software uses a fully implicit discretization and a coupled solver which uses an incomplete lower upper (ILU) factorization technique. The solver is accelerated using an algebraic multi-grid technique called additive correction. The standard k-ϵ turbulence closure was used for all simulations.

IV. Turbine Performance Parameters and Velocity Scale

It was necessary to characterize the turbine performance with respect to a reference velocity available to both CFD and basin-scale simulations. This requirement was somewhat problematic for two reasons. One was that the traditional performance parameters, thrust and power coefficients, rely on the 'freestream' velocity, which is not clearly defined in basin flows. The other is that the basin-scale simulation does not have sufficient resolution to provide a mean velocity through the turbine rotor (see figure 2 for an example grid resolution).

The approach was to represent the turbines in basin-scale simulations using two parameters, $C_T^\star$ and $C_P^\star$. These are

similar to the traditional thrust and power coefficients (C_T, C_P), except that instead of referring to the freestream velocity, a volume-averaged velocity ($\vec{u}_{\text{AV}}$) for a region containing the turbine is used. This was necessary because there is no clear definition for the freestream velocity in the context of a complex basin flow. The freestream velocity is only clearly defined when the flow is unbounded and the inflow is uniform, and therefore cannot be used in general.

A second option for the reference velocity would be to use the average velocity passing through the turbine rotor. Actuator disk theory defines this as $u_d = u_\infty(1-a)$ where a is the axial induction factor. This approach could be taken for CFD simulations because they have adequate resolution, however since the basin-scale simulation represents the turbine as a sub-grid-scale object, it cannot determine u_d explicitly and would thus need to use an empirical calibration.

The basin-scale model is formulated in terms of volume-averaged velocity for each grid cell. The chosen reference velocity must therefore be a volume-average over a region at least as large as the basin-scale model grid cells. Thus, an averaging volume (denoted by the subscript $_{\text{AV}}$) is introduced (see figure 2), and the volume-averaged velocity for this region is denoted $\vec{u}_{\text{AV}}$. The averaging volume may span multiple basin-scale grid cells.

$$\vec{u}_{\text{AV}} = \frac{\int_{\mathcal{V}_{\text{AV}}} \vec{u} d\mathcal{V}}{\int_{\mathcal{V}_{\text{AV}}} d\mathcal{V}} \tag{1}$$

This integration is evaluated numerically by both the CFD and basin-scale methods to give $\vec{u}_{\text{AVc}}$ and $\vec{u}_{\text{AVb}}$ respectively. For the general method to work, both CFD scale and basin-scale methods must provide a consistent prediction for ($\vec{u}_{\text{AV}}$).

The turbine performance parameters are defined by:

$$C_T^\star = \frac{T}{\frac{1}{2}\rho|\vec{u}_{\text{AVc}}|^2 A_f}, \qquad C_P^\star = \frac{P}{\frac{1}{2}\rho|\vec{u}_{\text{AVc}}|^3 A_f} \tag{2}$$

where T is the turbine thrust (axial force), P is the power output, ρ is the fluid density, and A_f is the frontal area of the turbine rotor.

V. Turbine Forces and Power

A. Basin-Scale

The horizontal grid resolution of the basin-scale simulations is larger than a turbine diameter, and therefore the forces of the turbine are distributed over a horizontal region in space which is larger than the actual turbine. However, many vertical layers of cells are often used to resolve variations in depth (figure 2). Thus, the turbine may span several vertical layers. For any grid cell in the basin-scale model, the turbine force per-unit-volume is specified by;

$$f_{\text{d,basin}} = -\frac{1}{2}\frac{A_{fc}}{\mathcal{V}_c}\rho C_T^\star |\vec{u}_{\text{AVb}}|\vec{u}_{\text{AVb}} \tag{3}$$

where A_{fc} is the portion of the turbine frontal area contained within the grid cell and $\mathcal{V}_c$ is the cell volume. For the example provided in figure 2, the turbine forces are distributed over cells 2 and 3, while $\vec{u}_{\text{AVb}}$ is calculated using cells 1,2,3 and 4.

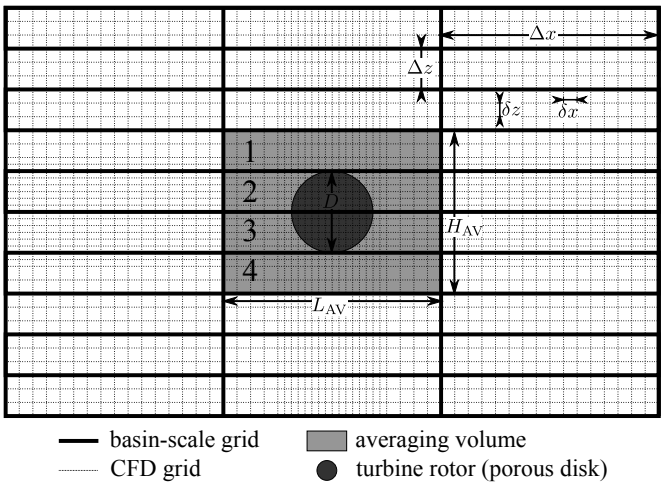

Fig. 2. Example of grid resolution for CFD and basin-scale simulations and definition of the velocity averaging volume. L_{AV} and H_{AV} refer to the averaging volume dimensions; Δx and Δz refer to the basin-scale grid; δx and δz refer to the device scale grid.

Conceptually, $f_{\text{d,basin}}$ is uniform over the rotor disk; however it's value may vary with depth due to variation in A_{fc}.

The basin-scale simulation calculates the power output using;

$$P_{\text{basin}} = \frac{1}{2}\rho|\vec{u}_{\text{AVb}}|^3 C_P^\star A_f \tag{4}$$

B. Device-Scale

In the CFD scale simulations, the representation of the turbines can range in complexity from full blade-resolved simulations, to simpler porous-disk type approaches. For the initial studies reported here, the porous disk approach has been used to provide a simplified representation of turbines. The porous disk method specifies the drag-per-unit-volume using;

$$f_{\text{d,cfd}} = -\frac{1}{2t_d}\rho K|u_x|u_x \tag{5}$$

where K is a non-dimensional resistance parameter, and t_d is the porous disk thickness in the CFD mesh. This type of specification allows the drag force to vary spatially over the disk. Such spatial variation may be present for turbines in boundary layers, or for non-uniform inflows due to local bathymetry or other turbines. This spatial variation was included in the CFD model because it has sufficient grid density to resolve its impacts, whereas the basin-scale model used a uniform drag distribution.

Note that it is possible to specify both axial and azimuthal (swirl) forcing terms for a spinning turbine rotor based on airfoil lift and drag coefficients. (Please see [6], [7] for more details). Such an approach may provide a more realistic representation of real turbines, however the present approach has been taken due to its relative simplicity.

The turbine thrust force T was found by numerically integrating $f_{\text{d,cfd}}$ over the porous disk volume region.

$$T = \int_{\mathcal{V}_{\text{disk}}} f_{\text{d,cfd}} \cdot d\mathcal{V} \tag{6}$$

Similarly, the power was found by numerical integration of the product of the local forcing term and local axial velocity.

$$P = \int_{\mathcal{V}_{\text{disk}}} f_{\text{d,cfd}} \cdot u_x \cdot d\mathcal{V} \tag{7}$$

This formulation gives an idealized power output which assumes that all of the applied force contributes directly to power production. Therefore blade drag and other losses are neglected. This was considered acceptable for these preliminary studies, but losses should be considered for more accurate power predictions. Note that the inclusion of such losses would be done at the device-scale and incorporated into the basin-scale model via reduced values for $C_P^\star$.

In general, $\vec{u}_{\text{AVc}}$, T and P are first determined from CFD simulation results to find $C_T^\star$ and $C_P^\star$, which are then passed to the basin-scale code and used in equation 3 for the applied drag and equation 4 for the output power.

VI. Simplified Channel Scenarios

The proposed methodology relies heavily on the assumption that the device-scale and basin-scale simulations will provide a consistent prediction of the volume-averaged velocity $\vec{u}_{\text{AV}}$. This consistency depends on the size of the averaging volume. Larger volumes will give better consistency but reduce the ability of the basin-scale simulation to resolve the flow. Much of the work done focused on determining an appropriate size for the averaging volume using simplified tidal channel scenarios to avoid the complexities of real basin flows.

The desired outcome was to achieve a high level of consistency between power estimates from the basin-scale and CFD simulations. Thus the target variable was the percent difference between the CFD prediction of power and the basin-scale prediction.

$$P_{\text{err}} = \frac{P_{\text{basin}} - P_{\text{cfd}}}{P_{\text{cfd}}} \tag{8}$$

Tests were performed with various representations of eddy viscosity, at different flow speeds, and with/without bottom friction. Additional tests were performed for a small array of turbines.

The channel was rectangular with length L=5 km, width W=1 km, and depth H=50 m. The basin-scale simulations specified the inlet mass flow rate as 50 000, 150 000 or 250 000 m^3/s (corresponding to inflow speeds of 1, 2 or 3 m/s, respectively). The water surface height was set to η=0 at the outlet. A single turbine was placed at mid-depth 25 m on the channel centreline 2 km from the inflow boundary. For the boundary layer tests, the turbine was placed at 35m depth. The turbine had a diameter of D=10 m. In the basin-scale simulations, two parameterizations for the vertical viscosity were examined, on was a constant ν_{v}=0.1 or 0.01 m^2/s, and the other used a k-ϵ closure.

In the CFD simulations, a portion of the channel surrounding the turbine(s) was modelled. Grid refinement studies were conducted according to the GCI_{OR} [8], [9] method and estimated discretization errors were less than 1% for thrust and power. Boundary conditions were set to maintain consistency with the basin-scale flow. The inlet was located 10D upstream of the turbine and the inflow velocity was either: uniform at 1,3 or 5 m/s; or a profile provided by results of the basin-scale simulation (for boundary layer cases). The inlet turbulence was set to *high* (10% intensity) which is thought to be reasonable for tidal channels. The domain spanned the full water depth (50 m). The top boundary used a rigid-lid assumption (fixed boundary, with free-slip condition). On the bottom, a free-slip condition was used except for the boundary layer cases, where the bottom shear stress was specified. The lateral boundaries were located 6D away from the turbine and used an *opening-for-entrainment* option, which approximates an infinite domain[2]. A pressure outlet was used with the reference pressure set to 0 Pa. Symmetry planes were used when applicable to reduce computational cost. The CFD simulations used the k-ϵ turbulence closure except when otherwise noted.

A. Convergence with vertical resolution

The first set of tests observed the change in P_{err} with increasing the vertical resolution (i.e. number of layers) of the basin-scale simulation. In the following discussion, the averaging volume dimensions have been normalized with respect to the turbine diameter D.

$$\hat{L}_{\text{AV}} = \frac{L_{\text{AV}}}{D} \qquad \hat{H}_{\text{AV}} = \frac{H_{\text{AV}}}{D} \tag{9}$$

For these tests, the averaging volume dimensions were $\hat{L}_{\text{AV}}$=4, $\hat{H}_{\text{AV}}$=1. The power error is shown in figure 3, where the x-axis $D/\Delta z$ represents the number of vertical layers per-turbine-diameter. Using a constant vertical viscosity of 0.1 m^2/s gave a convergent trend towards zero error. Using the k-ϵ closure produced a similar convergence trend, but towards -2% error. This reflects the fact that different coefficients are used in the k-ϵ closures for CFD and basin-scale models. Based on the observed trend, increasing $D/\Delta z$ from 4 to 16 (or greater) should only produce less than 2% discretization error. Therefore, $D/\Delta z$=4 (20 vertical layers for the 50 m deep channel) was typically used for the remainder of the studies.

B. Averaging volume horizontal size

The next set of tests observed the impact of changing the horizontal extent of the averaging volume. Tests were done using depth-averaged and 3D basin-scale simulations. Tests were done using $\hat{L}_{\text{AV}}$=1, 2 or 4, and are plotted in figure 4. Observing figure 4 it is apparent that the 2D depth-averaged case (H_{AV}=H) is the least sensitive to the averaging volume horizontal length-scale. For the 3D cases with 10 or 20 layers, $\hat{H}_{\text{AV}}$ was 1, and the sensitivity to $\hat{L}_{\text{AV}}$ was greater with increasing vertical resolution. Additionally, it can be seen that the sensitivity to the vertical resolution (# of

[2]Blockage effects are assumed negligible for all cases considered

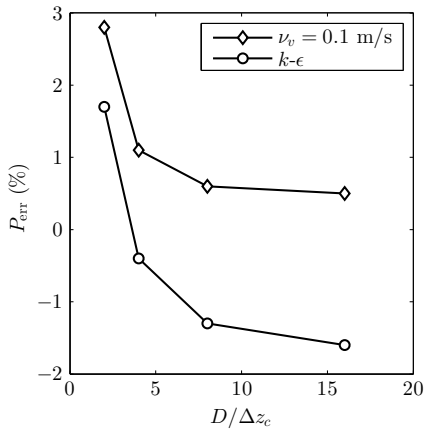

Fig. 3. Convergence trend with increasing vertical resolution of the basin-scale simulation, $D/\Delta z$ can be interpereted as the number of vertical layers per-turbine-diameter

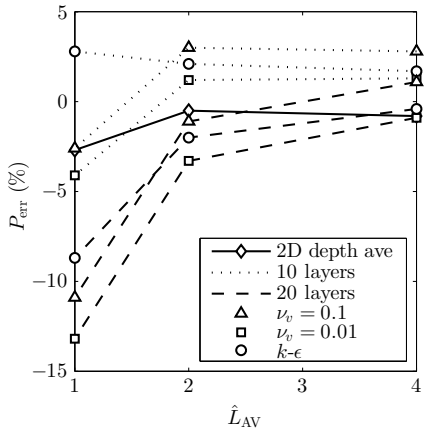

Fig. 4. Power error for set 1 tests ($\hat{H}_{\text{AV}}$=1)

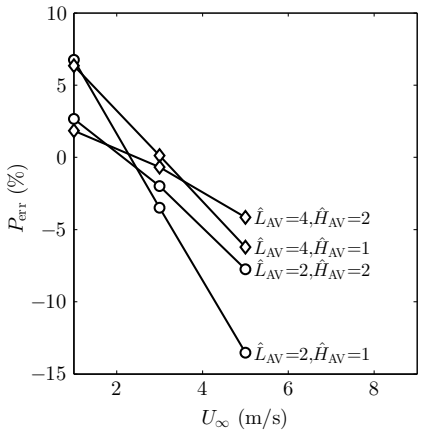

Fig. 5. Variation of power error with changing inflow velocity and averaging volume size, for a constant vertical viscosity A_v=0.1

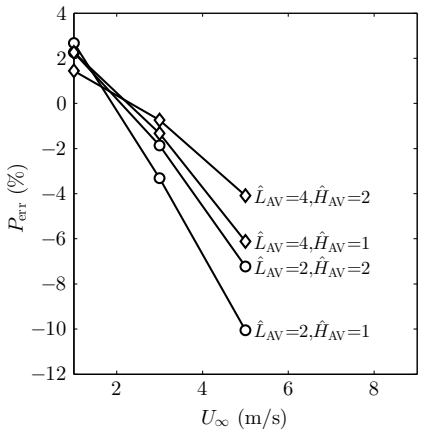

Fig. 6. Variation of power error with changing inflow velocity and averaging volume size, with vertical viscosity determined by the k-ϵ closure

layers) decreases as the averaging volume horizontal scale $\hat{L}_{\text{AV}}$ increases. In general, the consistency between CFD and basin-scale simulations improves with increasing averaging volume size. It was found that in general, $\hat{L}_{\text{AV}} = 1$ gave poor results and larger values were used for subsequent tests.

C. Inflow velocity and vertical size

A set of tests were conducted to validate the methodology over a range of inflow velocities covering expected values in real tidal channels (1, 3, and 5 m/s). Results are shown in figures 5 and 6. It was found that the basin-scale simulation tended towards under-predicting the power as the velocity increased. It is thought that this trend is partially due to differing treatments of turbulence between the two scales of simulation. Generally, the results improved with increasing the vertical and horizontal size of the averaging volume.

D. Boundary layer flows

A set of tests were conducted for simulations involving a boundary-layer. To ensure consistency between the two scales of simulation, the CFD model used a *specified shear* boundary condition for the bottom boundary instead of the typical no-slip condition. Also, to remove the impact of differing turbulence closures, some CFD simulations were run without a turbulence model but with the fluid viscosity set to be consistent with the total viscosity in the basin-scale simulations (i.e. ν_{cfd}=$\nu_{\text{t,basin}}$=0.1 m^2/s). For these constant viscosity cases, the friction velocity was $u^\star$=0.1344 m/s and the bottom shear stress was τ_b=18.063 Pa. In later simulations, the k-ϵ turbulence closure of each model was used to calculate the eddy viscosity.

The power error is plotted in figure 7. It was found that with sufficiently large averaging volumes, the basin-scale and device-scale simulations provided adequately consistent power estimates. This was true for both the constant viscosity, and k-ϵ cases. With $\hat{L}_{AV}$=1 or $\hat{H}_{AV}$=1, the power was not consistent between the two methods, particularly for the k-ϵ cases. Note that basin-scale simulations often include source terms for turbulence that are associated with form drag, however it was found that such sources needed to be disabled to obtain consistent results.

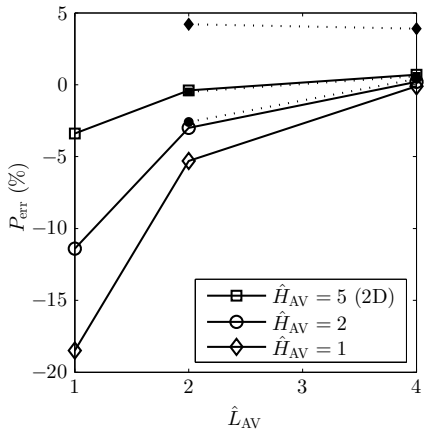

Fig. 7. Power error for boundary layer tests, unfilled symbols are for cases with constant vertical viscosity, filled symbols are for the k-ϵ turbulence model

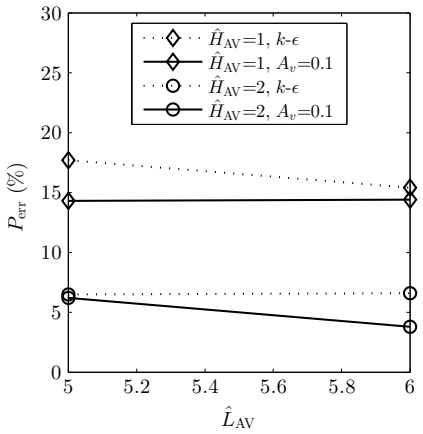

Fig. 9. Power error for array tests

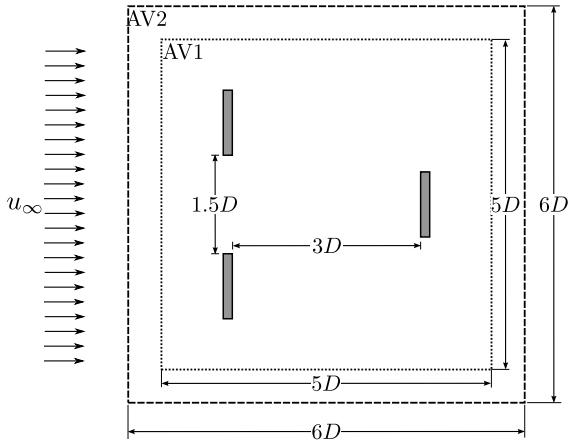

Fig. 8. Layout of turbines for the small array test case

E. Array tests

The final set of tests done using the simple channel scenario was for a simple array of turbines with uniform inflow. The CFD simulations used the k-ϵ turbulence model in all cases, while the basin-scale model was tested using both k-ϵ and constant ν_v=0.1 m^2/s. The layout of the turbines is depicted in figure 8. The power error is plotted in figure 9. The power discrepancy was approximately 6% with $\hat{H}_{\text{AV}}$=2 and $\hat{L}_{\text{AV}}$=5 or 6.

Attempts were also made to use a separate averaging volume for each individual turbine in the array but it was found that the basin-scale model could not resolve the interaction effects between the turbines adequately, so the impact of the three turbines needed to be lumped together into a single basin-scale element.

F. Summary

All of the tests indicated that the averaging volume size should be least twice the dimension of the turbine (or array of turbines) in order to maintain consistency with the device-scale simulations. Physically, the volume should average-out the differences between the hydrostatic basin-scale model and non-hydrostatic CFD model. Typical errors range up to 7%. The general degree of accuracy holds across the velocity range typical for operation of turbines with higher errors at high velocity.

Reducing the size of the averaging volume leads to substantial errors due to differences in the flow around the turbine caused by formulation differences between the Ocean and CFD model.

The k-ϵ turbulence closure model yields a more realistic and accurate calculation of vertical viscosity and its important horizontal and vertical variations. It also produces more realistic turbine wake recovery. However, it was found that typical turbulence sources associated with form drag had to be disabled to obtain power results consistent with the CFD simulatouins.

VII. Minas Passage

The simplified channel scenarios gave some insight into the behaviour of the method, however a more realistic scenario was also pursued to determine the feasibility for real-world scenarios. The chosen site was the FORCE test site in Minas Passage in the Bay of Fundy. At this preliminary stage, it has been assumed that the turbine performance parameters $C_T^\star$ and $C_P^\star$ remain constant over the tidal cycle. In reality, they would vary somewhat with the inflow velocity and direction and due to limitations in real turbine operation such as cut-in speed.

A. Site characteristics

The Bay of Fundy is located on the east coast of North America between approximately 44° and 46° N latitude (figure 10). The resonant period of this system is slightly longer than the period of the dominant M2 tidal constituent and this area is well known for the large tide range in the upper bay. The node point for the oscillation is near the shelf break east of Georges Bank; however, this is complicated by other resonances parallel to the shelf that extend down to Boston and Cape Cod.

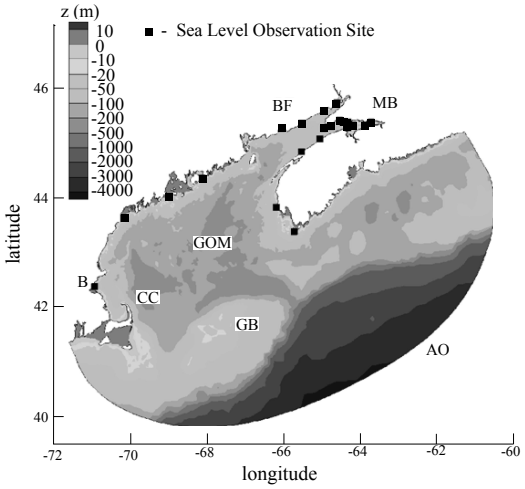

Fig. 10. Bathymetry for the Bay of Fundy region. AO - Atlantic ocean; GOM - Gulf of Maine; BF - Bay of Fundy; MB - Minas Basin; GB - Georges Bank; B - Boston; CC - Cape Cod

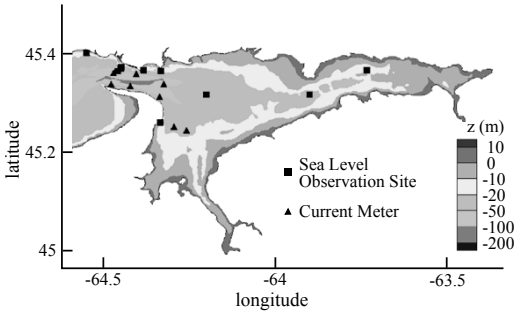

Fig. 11. Bathymetry for the Minas Basin

For several reasons, the entire bay down to Cape Cod and extending offshore has been modelled in this study. For one, modifying the form drag in the upper bay can alter the resonance so that it becomes difficult to specify boundary conditions in a more limited area model. Moreover, previous studies have shown that introducing features such as barrages

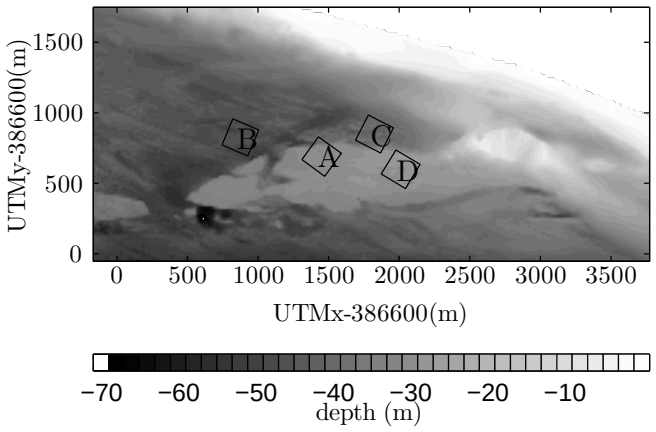

Fig. 12. Bathymetry for the region around the test berths

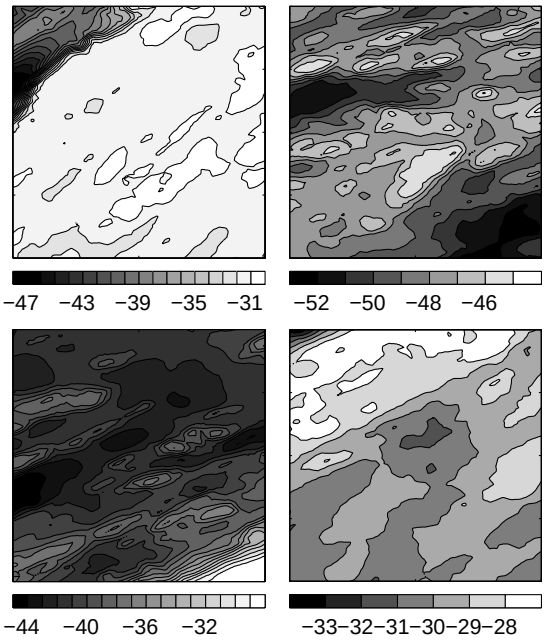

Fig. 13. Bathymetry for the 200×200 m CFD subdomains (x aligned with flow direction at peak flood). Berth A (top left), B (top right); C (bottom left); D (bottom right). Depths are in meters relative to chart datum (approx 6m below MSL)

can modify the resonance and have significant effects on tides as far as Boston [10]. The particular areas of interest were Minas Basin where the largest tide range occurs, and Minas Passage that connects Minas Basin with the upper Bay of Fundy (figure 11). The region contains extensive tidal flats, and sensitivity tests indicated that treating wetting and drying of these flats accurately is important for attaining accurate model results for velocity amplitude and phase.

The dominant tidal constituent is the M2 and the amplitude varies from 0.5 m at the open boundary to over 6 m in Minas Basin. In an earlier study, 8 constituents were used in the open boundary conditions (M2, S2, N2, K2, K1, O1, P1, Q1). Most of these constituents are small compared to the M2 (particularly the diurnal constituents) but were retained in order to assess the accuracy of the model against tide and current observations. The nonlinear interactions between the semi-diurnal constituents are important in many situations. The earlier results indicated that this representation of the system was reasonably accurate with constituent amplitude errors of a few cm and phase errors of a few degrees in general.

B. Device-scale Simulations

There are plans for four berths at the FORCE test site for demonstration turbines . The present study used simplified turbines located at these sites. For each berth, a CFD sub-domain was created aligned with the expected flow at the maximum flood condition from basin-scale simulations with no turbine forcing present (see figure 12). The sub-domains were 200×200 m, and the bottom boundary was generated using 5 m resolution bathymetry data [11] (figure 13). The

upper boundary location was set using the initial basin-scale simulation results for depth at the centre of the sub-domain for the max-flood condition. The sub-domains were discretized using the same meshing strategy as for the simple channel cases, except that the elements conformed to the irregular bottom geometry. For all cases, a generic turbine with D=16 m was used for each berth. The porous disk resistance coefficient was set to a value of K=1.8. The turbines were placed at mid-depth in the centre of each sub-domain. The boundary conditions for the CFD simulations were set using output data from the basin-scale model.

1) *Inflow:* At the upstream boundary (inlet) the velocity was specified using a 2D cubic interpolation of the nodal values from the basin-scale grid. This interpolation was done with respect to the lateral position (y) along the boundary, and the height (h) above the bottom[3]. The inlet turbulent kinetic energy k and dissipation rate ϵ were set using a 2D linear interpolation (with respect to y and h) of the face-centred values output from basin-scale simulations.
2) *Sides:* At the lateral boundaries, an *opening* condition was specified. For cases with inflow through the boundary (i.e. when the flow was yawed relative to the grid), the velocity and turbulence quantities were set using the same interpolation methods as for the inlet. For cases where there was no inflow through the boundary (all outflow) the *opening for entrainment* option was used with zero relative pressure and zero-gradient conditions for k and ϵ.
3) *Bottom:* Along the bottom boundary, the shear stress was specified using a linear interpolation of face-centred values from the basin-scale simulation. The shear stress was specified in this manner to ensure consistency between the two models.
4) *Top:* The top boundary used a *rigid lid* approximation, with a constant-height, free-slip wall. The height of the boundary was set based on the basin-scale model prediction at the domain centre. Note that since the water surface height is different at different phases of the tidal cycle, the present methodology requires a different mesh for each phase being simulated. Additionally, a new mesh is also required for each iteration of the overall tuning loop (see figure 1) since the surface height may change with each iteration.
5) *Outlet:* A pressure outlet with zero relative pressure was used.

It is of interest to note that due to the spatial interpolations employed, the inflow conditions specified at the domain boundaries were not guaranteed to be perfectly compatible with the RANS equations. It was found that the iterative convergence of residual values was affected by this near the inflow boundaries. Thus, iterative convergence was assessed by observing trends in velocity at several points within the domain (concentrated in the wake of the turbine). In post-processing, the rms and max residuals were verified within a region offset by 20m from the inflow conditions. It was verified that the rms residuals converged by 6 orders within this region. The values of $C_T^\star$ and $C_P^\star$ were then calculated from the converged flowfield.

[3]Using the depth below mean-sea-level for the interpolation instead of h resulted in non-physical velocity profiles at the bottom boundary due to better resolution of the irregular bottom by the CFD grid compared to the basin-scale grid

C. Basin-Scale Simulations

The grid was constructed from unstructured triangles that varied in edge length from 12 km on the open boundary to 40 m at the berth sites. In total, there were 69 583 vertices and 135 101 triangular elements in the horizontal. Two types of simulations were run; depth-averaged (2D); and 3D flow resolved using 24 terrain-following layers. The layer spacing was refined near the bottom to resolve the boundary layer. On a desktop computer, the model ran 60 times faster (2D) and 15 times faster (3D) than simulated time. The domain extended down to Cape Cod and far offshore. The flow was driven by the M2 tidal forcing.

Initially the basin model was run with approximate turbine parameter values to provide boundary conditions to the CFD model. The CFD model was then used to recalculate the turbine parameters. The basin model was then re-run with the updated turbine parameters. The CFD simulation was then re-run and the output $C_T^\star$ and $C_P^\star$ were checked against the previous run to determine if further iteration was necessary. For all berths, a single iteration was sufficient to achieve converged results for $C_T^\star$ and $C_P^\star$.

D. Model Results

As with the simple channel tests, the consistency between the CFD and basin-scale power estimates was of key concern. It was found that with the increased complexity of the flows, there was a greater discrepancy in $\vec{u}_{\mathrm{AV}}$. Table I summarizes the turbine performance parameters and power output from CFD and basin-scale simulations.

The FORCE test site scenario tested here is a significantly more complex problem, however the power predictions remain consistent within 16% for 2D simulations and within 26% for the 3D simulations for each considered berth location. Note that since the power is proportional to the cube of the velocity, even small discrepancies in the averaged velocity lead to large discrepancies in power. The CFD models are driven with boundary conditions derived from the basin model, but even within the small sub-domain the models are resolving the flow differently. This is most pronounced for the 3D simulation of Berth A, where most of the sub-domain sits on a ledge of about 32 m depth. But in the north portion of the domain the bottom falls down to about 50 m depth. Current speed is highly variable within the sub-domain; even when simulated without the presence of a turbine there is an estimated 10 cm/s difference in flow speed across the face of the averaging volume. The different resolutions and physics between the models result in different estimates of the flow field and therefore different estimates of velocity and power at the turbine.

Testing with a range of inlet conditions has shown the turbine parameters $C_T^\star$ and $C_P^\star$ to be quite stable. This suggests that any discrepancy in the flow field between the CFD and basin model will have little impact on the values of $C_T^\star$ and $C_P^\star$. The turbine power is much more sensitive to the current speed. The difference in power estimates comes down to the consistency of the velocity estimates of each model.

VIII. Conclusions

This paper has presented a methodology for representing turbines in basin-scale simulations based on performance metrics obtained from CFD simulation results. A major challenge for such modelling is choosing how to parameterize the turbine performance. The standard thrust and power coefficients are of little value since it is not possible to define a freestream velocity for such flows. This paper proposes using a volume-averaged velocity $\vec{u}_{\text{AV}}$ taken from a region large enough that CFD and basin-scale simulations give a consistent value of $\vec{u}_{\text{AV}}$. The thrust and power are then normalized using this average velocity.

Simple channel scenarios showed fairly good agreement for power (within 7% or less) when the averaging volume is a cube with side-lengths roughly twice the turbine diameter. Using larger volumes resulted in better consistency for the simple cases.

The complex Minas passage cases were more challenging and good consistency was not achieved in general. Two dimensional basin-scale simulations produced peak-flood power consistent within about 16% to CFD simulations.

An advantage of the volume-averaging method is that it allows the CFD model to do what it does best in modelling the small-scale flow accurately, and allows the ocean model to do what it does best in efficiently modelling the large-scale flows. For given power conditions, the coefficients $C_T^\star$ and $C_P^\star$ are relatively constant over a range of current speeds so that the method is robust.

To achieve agreement in power estimates between the basin-scale and CFD models in complex scenarios such as this, further work is required. Possible improvements may be achieved by making the formulation for bottom friction consistent between the models, modifying the turbulence closures to be more consistent or to include free surface effects in the CFD model. As it stands, the methodology is adequate for rough power predictions, but greater confidence would be gained with better consistency to CFD results for power.

The results presented here highlight the difficulty in modelling tidal turbines in-situ. It is relatively easy to perform simulations of idealized flows, but real tidal flows are vastly more complex. It may be that a tighter coupling between basin-scale models and CFD scale models is required, where the two models are solved simultaneously with shared boundaries. This approach is currently being considered at the University of Victoria.

Acknowledgment

The authors thank the Offshore Energy Research Association of Nova Scotia (OERA) for financial support.

TABLE I
CFD and basin-scale power (kW) at peak flood

Berth	$\hat{L}_{\text{AV}}$	$\hat{H}_{\text{AV}}$	$C_T^\star$	$C_P^\star$	P_{cfd}	P_{basin}	% diff
A	2.5	>2	1.031	0.767	990	1117	13%
B	4.7	>2	0.988	0.727	1501	1266	-16%
C	4.7	>2	1.002	0.739	1424	1284	-10%
D	2.5	>2	1.020	0.761	1350	1397	3%
A	2.5	2	1.080	0.822	990	1249	26%
B	4.7	2	0.995	0.734	1501	1220	-19%
C	4.7	2	0.981	0.716	1424	1249	-12%
D	2.5	2	1.072	0.821	1350	1456	8%

References

[1] R. H. Karsten, J. M. McMillan, M. J. Lickley, and R. D. Haynes, "Assessment of tidal current energy in the minas passage, bay of fundy," *Proc. IMechE Vol. 222 Part A: J. Power and Energy*, vol. 222, pp. 493–507, 2008.

[2] R. Walters and V. Casulli, "A robust, finite element model for hydrostatic surface water flows," *Communications in Numerical Methods in Engineering*, vol. 14, pp. 931–940, 1998.

[3] R. Walters, "Design considerations for a finite element coastal ocean model," *Ocean Modelling*, vol. 15, pp. 90–100, 2006.

[4] R. Walters and D. Plew, "Numerical modeling of environmental flows using dam: Some preliminary results," *Acta Geophysica*, vol. 56, pp. 918–934, 2008.

[5] R. Walters, E. Hanert, J. Pietrzak, and D. Le Roux, "Comparison of unstructured, staggered grid methods for the shallow water equations," *Ocean Modelling*, vol. 28, pp. 106–117, 2009.

[6] R. Mikkelsen, "Actuator disc methods applied to wind turbines," Ph.D. dissertation, University of Denmark, 2003.

[7] M. Shives, "Hydrodynamic modeling, optimization and performance assessment for ducted and non-ducted tidal turbines," Master's thesis, University of Victoria, 2011.

[8] I. Celik, U. Ghia, P. Roache, C. Freitas, H. Coleman, and P. Raad, "Procedure for estimation and reporting of uncertainty due to discretization in cfd applications," *Journal of Fluids Engineering*, vol. 130, 2008.

[9] T. Xing and F. Stern, "Closure to discussion of factors of safety for richardson extrapolation (2011, asme j. fluids eng., 133, p. 115501)," *Journal of Fluids Engineering*, vol. 133, pp. 1–6, 2011.

[10] P. V. Sucsy, B. R. Pearce, and V. G. Panchang, "Comparison of two- and three-dimensional model simulation of the effect of a tidal barrier on the gulf of maine tides," *Journal of Physical Oceanography*, vol. 130, pp. 114–118, 1993.

[11] D. R. Parrott, B. J. Todd, J. Shaw, J. E. H. Clarke, J. Griffin, B. MacGowan, M. Lamplugh, and T. Webster, "Integration of multibeam bathymetry and lidar surveys of the bay of fundy, canada," in *Proceedings of the Canadian Hydrographic Conference and National Surveyors Conference*, 2008.

View publication stats